74rd International Astronautical Congress (IAC), Baku, Azerbaijan, 2-6 October 2023.

IAC-23,D1,4B,11,x79870

Optimal Orbital Configurations of Spaceborne Optical Sensors Constellations for Space Surveillance

Antonio D'Anniballe[a]*, Leonard Felicetti[a], Stephen Hobbs[a]

[a] Cranfield University, United Kingdom, antonio.danniballe@cranfield.ac.uk
* Corresponding author

Abstract

With the increasing number of satellites, there is a progressively higher demand for accurate surveillance and collision risk analysis systems. Most of the space situational awareness domain depends today on ground-based telescopes and radar sensors, which have the disadvantage of being highly constrained in terms of their potential geographic positions. A more versatile approach may instead be the use of a constellation of spacecraft carrying space-based sensors that can cover any desired orbital region allowing for complete coverage of the orbiting population, enabling a more accurate orbit estimation and consequent collision risk analysis. This work investigates the optimal orbital configurations of a LEO constellation of satellites carrying optical sensors when these are used for the orbit estimation and the conjunction assessment of resident space objects. Orbit estimation is performed through covariance analysis using unscented transform techniques and unscented Kalman filtering. The optimal configuration of the constellation is found using nonlinear optimization techniques, maximizing the performance in terms of number of available sensors over a given time window. The optimization is carried on for two different population, one orbiting the LEO region with random orbital parameters, and the other located in a narrow range of right ascension and inclination values. The results inform on how to optimally deploy constellations of satellites carrying optical sensors for surveillance and collision assessment of uncooperative spacecraft and on the effect that the number of constellation satellites has on performance.

Keywords: space situational awareness, orbit estimation, constellation, optical sensors

1. Introduction

In the past few years the number of launches to LEO has increased significantly. Once objects are in space, degradation and collisions with other objects causes fragmentation. The generated fragment orbit at high velocity, and may pose a risk to operational satellites. When debris are too big, they are dangerous to operators, and can contribute to the unstable evolution of the debris environment harming future missions [1]. To be able to accurately forecast the future of the space debris environment, to quantify the risks it poses, and to guarantee informative and timely conjunction data messages, it is paramount to be able to accurately determine the state of such objects at all times. Currently, objects in LEO are observed mostly through radar stations on Earth, usually part of big global ground-based space surveillance networks such the EU SST [2]. Such ground networks employ hundreds of sensors of variable size and accuracy. However, these sensors can't be deployed uniformly on Earth. Geographical and political constraints limit where a measurement station can be built, which in turns limits the timely coverage of orbital regions. Moreover, ground networks are usually the results of cooperation between many different entities that ought to closely cooperate to guarantee an effective service, a condition which is expensive to maintain and is subject to the maintaining of healthy relationships between institutions. A solution to these issues could be represented by space-based constellations of spacecraft carrying payload for space surveillance and tracking, capable of processing data, communicating with each other, and linked only to a limited number of ground stations. As there are currently some operational space surveillance spacecraft such as the Canadian Sapphire contributing to the US SSN, this solution seems technologically feasible in the near future [3].

In this paper, a study for a constellation of spacecraft carrying optical sensors for space surveillance is presented. The work focuses on evaluating the potential advantages of such a constellation when compared to a ground-based network. Moreover, a methodology for finding the optimal parameters of such a constellation with respect to some performance metric is presented.

In the following sections, a parametrization for the constellation is formally defined, together with a characterization of the population of debris targeted by the surveillance system, also called target population. A model for the sensors is then presented, together with the relevant assumptions. The algorithms used for orbit propagation and estimation are then discussed, along with the methodology for the optimization procedure. The results of the optimization procedure against the number of spacecraft in the constellation is then shown and discussed, providing insight on the preliminary design and potential limitations of such a surveillance system.

2. Model Definition

In this section, the analysed scenario is presented, including the assumptions for the target population and the parametrization of the sensor constellation. The sensor models are described, with a brief description of the underlying key assumptions.

2.1. Scenario

Two different population of N_t targets are considered. In the first case, all the targets are assumed to be objects in LEO, with altitudes between 600 and 1200 km, moving in circular orbits of random inclinations and right ascensions of the ascending node. This population will be referred to as *random population*. In the second case, the random targets lie within the same altitude range, but are constrained at 98 deg inclination and to a right ascension between 0 deg and 10 deg, effectively lying in a slice of the sky. This population will be referred to as *SSO limited population*. In both cases, the targets have random ballistic coefficients between 0.2 and 20 m^2/kg. These are relatively high values chosen to make the effect of atmospheric drag non-negligible over short time windows.

The orbits of the targets within this population are estimated using the measurements of a constellation of spacecraft carrying optical sensors. The constellation of optical sensors is assumed to orbit the LEO region as well. The constellation assumes N_{SAT} spacecraft carrying optical sensors evenly distributed over N_o orbits in a Walker-like configuration [4]. Each orbit is assumed to be circular, at the same altitude and at the same inclination and in a radially symmetric configuration with respect to the right ascension of the ascending node. The first orbital plane is defined using its right ascension of the ascending node as an additional parameter. Then, for every spacecraft in the constellation:

$$in_{i,k} = in_k,\ i = 1 : \frac{N_{SAT}}{N_o},\ k = 1 : N_o \tag{1}$$

$$\Omega_{i,k} = \Omega_0 + \frac{2\pi(k-1)}{N_o},\ i = 1 : \frac{N_{SAT}}{N_o},\ k = 1 : N_o \tag{2}$$

$$\nu_{i,k} = \frac{2\pi(i-1)N_{SAT}}{N_o},\ i = 1 : \frac{N_{SAT}}{N_o},\ k = 1 : N_o \tag{3}$$

where i is the index associated to the spacecraft within the constellation orbit, k is the index associated to the constellation orbit, in_k is the provided inclination for the constellation orbits, Ω_0 is the right ascension of the first orbital plane, and ν is the true anomaly. This parametrization is chosen to minimise the number of parameters while retaining a non-trivial set of configurations. A summary of the constellation parameters can be found in Table 1.

Table 1: Constellation Parameters

Parameter	Symbol
Number of spacecraft per orbit [-]	$N_{SC/ORB}$
Number of orbits [-]	N_o
RAAN of first orbit [deg]	Ω_o
Inclination [deg]	in
Altitude [km]	h

The targets are also observed by a ground network of six radar stations mimicking existing surveillance networks such as EU SST. The precise locations used for the ground stations can be found in Table 2.

Table 2: Ground Stations

Location	Long [deg]	Lat [deg]
United Kingdom	0.0	51.0
Spain	-6.0	38.0
United States	-115.0	33.0
Chile	-69.0	-23.0
South Africa	20.0	-33.0
New Zealand	170.0	-44.0

The following assumptions hold:

- The population follows natural perturbed dynamics.
- The constellation spacecraft are kept in their initial orbits via periodic station-keeping manoeuvres.
- Both the constellation and the ground network are always operational.

2.2. Sensor Models

The radar and optical sensor models are derived from purely geometrical transformations. Given a target position vector in Earth Centred Inertial (ECI) frame $\mathbf{r}_T = [x_T,\ y_T,\ z_T]^T$ and a sensor position vector $\mathbf{r}_S = [x_S,\ y_S,\ z_S]^T$, we have:

$$\rho = \sqrt{(x_T - x_S)^2 + (y_T - y_S)^2 + (z_T - z_S)^2} \tag{4}$$

$$\theta = arccos\frac{z_T - z_S}{\rho} \tag{5}$$

$$\phi = sgn(y_T - y_S)arccos\frac{x_T - x_S}{\rho} \tag{6}$$

where ρ is the range, θ the elevation component, and ϕ is the azimuthal component. The observation functions for the optical and the radar sensor will then be:

$$\mathbf{h}_{opt} = \mathbf{h}_{opt}(\mathbf{r}_T) = [\theta(\mathbf{r}_T) + n_\theta,\ \phi(\mathbf{r}_T) + n_\phi]^T \tag{7}$$

$$\mathbf{h}_{rad} = \mathbf{h}_{rad}(\mathbf{r}_T) = [\rho(\mathbf{r}_T),\ \theta(\mathbf{r}_T),\ \phi(\mathbf{r}_T)]^T \quad (8)$$

with measurement outputs:

$$\mathbf{y}_{opt} = \mathbf{h}_{opt}(\mathbf{r}_T) + \mathbf{n}_{opt} \quad (9)$$

$$\mathbf{y}_{rad} = \mathbf{h}_{rad}(\mathbf{r}_T) + \mathbf{n}_{rad} \quad (10)$$

where $\mathbf{n}$ is a Gaussian random variable with zero mean and diagonal covariance matrix representing the noise component of the measurement. In this work it is assumed that the standard deviation on the range $\sigma_{n,\rho}$ is 10 m and the standard deviations on the angles $\sigma_{n,\theta}$, $\sigma_{n,\phi}$ are 5 arcsec.

Measurements are only collected whenever some visibility conditions are satisfied. In particular, the target should be within the field of view of the radar sensor and illuminated by the sun such that it is visible for the optical sensors. Such conditions include:

- Visibility of target from radar sensor, expressed analytically as:

$$arccos\frac{(\mathbf{r}_T - \mathbf{r}_S)\cdot\mathbf{r}_S}{\|\mathbf{r}_T - \mathbf{r}_S\|\|\mathbf{r}_S\|} < FOV/2 \quad (11)$$

  where FOV is the field of view of the radar sensor.

- Visibility of target from optical sensor, accounting for obstruction of the Earth. Analytically [5]:

$$\sqrt{\frac{r_S^2 r_T^2 - (\mathbf{r}_T\cdot\mathbf{r}_S)^2}{r_S^2 + r_T^2 - 2\mathbf{r}_T\cdot\mathbf{r}_S}} - R_E > 0 \quad (12)$$

  where R_E is the Earth radius.

- Illumination of target from the Sun, expressed as:

$$arccos\frac{(\mathbf{r}_S - \mathbf{r}_T)\cdot(\mathbf{r}_S - \mathbf{r}_{SUN})}{\|\mathbf{r}_T - \mathbf{r}_S\|\|\mathbf{r}_S - \mathbf{r}_{SUN}\|} < \frac{\pi}{2} \quad (13)$$

  where $\mathbf{r}_{SUN}$ is the Sun-Earth vector. This expression verifies that the phase angle α, as shown in Fig. 1, is below 90 deg.

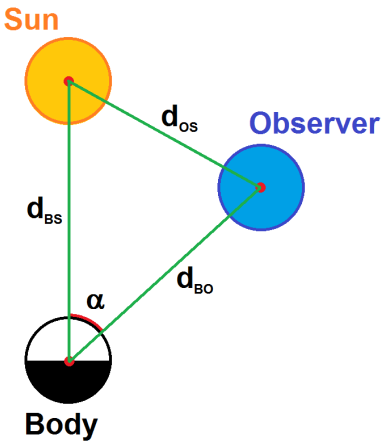

Figure 1: Phase angle for target visibility [6]

Moreover, the following assumptions hold:

- Measurements are taken continuously.
- Measurements data is sent to the ground processor for orbit estimation without delay.
- Optical payload carried by the constellation spacecraft is such that all the visible targets are captured irrespective of spacecraft attitude.
- Targets are efficiently tracked and measurement association is done instantaneously with 100% accuracy.
- The accuracy of any sensor is not dependent on range.
- All radar sensors have a high FOV of 70 deg. This takes into account the fact that a single radar station has multiple radar sensors in place to cover a broad sky area.

3. Performance Assessment Methodology

In this section, the methodology of the study is explained in detail. First, the analysed scenario is presented, including the set-up for the target population and the parametrization of the sensor constellation. First, the orbit propagation model is described. Next, the sequential orbit estimation model is presented. The algorithm for retrieving the estimation data is then explained. Finally, the algorithm for the optimization is explained along with a definition of the target performance metric.

3.1. Orbit Propagation

The propagation model follows the perturbed two-body problem equations accounting for atmospheric drag

and Earth oblateness effect. For an orbiting target with position vector $\mathbf{r} = [x\ y\ z]^T$, it holds [7]:

$$\ddot{\mathbf{r}} = -\frac{\mu}{r^3}\mathbf{r} + \mathbf{a}_{J2} + \mathbf{a}_D \tag{14}$$

where μ is the Earth gravitational parameter. The perturbing accelerations are:

$$\mathbf{a}_{J2} = \frac{3}{2}\frac{J_2 R_E^2}{r^5}\begin{bmatrix}(5\frac{z^2}{r^2}-1)x\\(5\frac{z^2}{r^2}-1)y\\(5\frac{z^2}{r^2}-3)z\end{bmatrix} \tag{15}$$

$$\mathbf{a}_D = -\frac{1}{2}\frac{C_D A \rho}{M} v\mathbf{v} \tag{16}$$

where J_2 is the spherical harmonic coefficient of order (2,0) for the Earth's gravitational field, C_D is the drag coefficient, A is the target cross-section, M is its mass, ρ is the atmospheric density and $\mathbf{v}$ is the velocity vector.

3.2. Unscented Kalman Filter

The orbit estimation strategy employs an Unscented Kalman Filter (UKF). Provided the known initial state and covariance for each target, one has:

$$\mathbf{x}_0 = [\mathbf{r}_0^T,\ \mathbf{v}_0^T]^T \tag{17}$$

where $\mathbf{r}_0$ is the initial position and $\mathbf{v}_0$ is the initial velocity of the target, with $\mathbf{x}_0$ initial state and $\mathbf{x}_k$ the state at timestep t_k. An initial covariance $\mathbf{P}_0$ is supplied as well, such that:

$$\mathbf{P}_0 = diag(\mathbf{P}_{r,0}, \mathbf{P}_{v,0}) = diag(\sigma_{r,0}^2\mathbf{I}_{3x3},\ \sigma_{v,0}^2\mathbf{I}_{3x3}) \tag{18}$$

with $\mathbf{I}$ identity matrix, assuming $\sigma_{r,0} = 10$ m, $\sigma_{v,0} = 0.1$ m/s for all targets. Then, the UKF follows the algorithm shown in Fig. 2.

In particular, the state propagator follows a first order forward scheme, such that, given a dynamical system:

$$\dot{\mathbf{x}} = \mathbf{f}(\mathbf{x}) \tag{19}$$

for each sigma point:

$$\mathbf{x}_k = \mathbf{x}_{k-1} + (t_k - t_{k-1})\mathbf{f}(\mathbf{x}_{k-1}). \tag{20}$$

At timestep t_k, for each target, the measurement vector will contain all available measurements stacked on a single vector of size $2N$ or $3N$, depending on whether we are using the ground network or the constellation for estimation, where N is the number of available measurements, with corresponding measurement covariance of size $2Nx2N$ or $3Nx3N$:

$$\mathbf{y}_{const,k} = [\mathbf{y}_{opt,k}^{1\,T}, \dots, \mathbf{y}_{opt,k}^{N\,T}]^T \tag{21}$$

$$\mathbf{y}_{gnd,k} = [\mathbf{y}_{rad,k}^{1\,T}, \dots, \mathbf{y}_{rad,k}^{N\,T}]^T. \tag{22}$$

If all visibility checks fail, and therefore no measurement will be available, the Kalman gain will collapse to zero and the UKF will act as a state and uncertainty propagator.

Initialize with:

$$\hat{\mathbf{x}}_0 = E[\mathbf{x}_0]$$
$$\mathbf{P}_0 = E[(\mathbf{x}_0 - \hat{\mathbf{x}}_0)(\mathbf{x}_0 - \hat{\mathbf{x}}_0)^T]$$
$$\hat{\mathbf{x}}_0^a = E[\mathbf{x}^a] = [\hat{\mathbf{x}}_0^T\ \mathbf{0}\ \mathbf{0}]^T$$

$$\mathbf{P}_0^a = E[(\mathbf{x}_0^a - \hat{\mathbf{x}}_0^a)(\mathbf{x}_0^a - \hat{\mathbf{x}}_0^a)^T] = \begin{bmatrix}\mathbf{P}_0 & \mathbf{0} & \mathbf{0}\\ \mathbf{0} & \mathbf{P_v} & \mathbf{0}\\ \mathbf{0} & \mathbf{0} & \mathbf{P_n}\end{bmatrix}$$

For $k \in \{1, \dots, \infty\}$,

Calculate sigma points:

$$\boldsymbol{\mathcal{X}}_{k-1}^a = \left[\hat{\mathbf{x}}_{k-1}^a\ \ \hat{\mathbf{x}}_{k-1}^a \pm \sqrt{(L+\lambda)\mathbf{P}_{k-1}^a}\right]$$

Time update:

$$\boldsymbol{\mathcal{X}}_{k|k-1}^x = \mathbf{F}[\boldsymbol{\mathcal{X}}_{k-1}^x, \boldsymbol{\mathcal{X}}_{k-1}^v]$$
$$\hat{\mathbf{x}}_k^- = \sum_{i=0}^{2L} W_i^{(m)} \mathcal{X}_{i,k|k-1}^x$$
$$\mathbf{P}_k^- = \sum_{i=0}^{2L} W_i^{(c)} [\mathcal{X}_{i,k|k-1}^x - \hat{\mathbf{x}}_k^-][\mathcal{X}_{i,k|k-1}^x - \hat{\mathbf{x}}_k^-]^T$$
$$\boldsymbol{\mathcal{Y}}_{k|k-1} = \mathbf{H}[\boldsymbol{\mathcal{X}}_{k|k-1}^x, \boldsymbol{\mathcal{X}}_{k-1}^n]$$
$$\hat{\mathbf{y}}_k^- = \sum_{i=0}^{2L} W_i^{(m)} \mathcal{Y}_{i,k|k-1}$$

Measurement update equations:

$$\mathbf{P}_{\mathbf{y}_k\mathbf{y}_k} = \sum_{i=0}^{2L} W_i^{(c)} [\mathcal{Y}_{i,k|k-1} - \hat{\mathbf{y}}_k^-][\mathcal{Y}_{i,k|k-1} - \hat{\mathbf{y}}_k^-]^T$$
$$\mathbf{P}_{\mathbf{x}_k\mathbf{y}_k} = \sum_{i=0}^{2L} W_i^{(c)} [\mathcal{X}_{i,k|k-1} - \hat{\mathbf{x}}_k^-][\mathcal{Y}_{i,k|k-1} - \hat{\mathbf{y}}_k^-]^T$$
$$\mathcal{K} = \mathbf{P}_{\mathbf{x}_k\mathbf{y}_k}\mathbf{P}_{\mathbf{y}_k\mathbf{y}_k}^{-1}$$
$$\hat{\mathbf{x}}_k = \hat{\mathbf{x}}_k^- + \mathcal{K}(\mathbf{y}_k - \hat{\mathbf{y}}_k^-)$$
$$\mathbf{P}_k = \mathbf{P}_k^- - \mathcal{K}\mathbf{P}_{\mathbf{y}_k\mathbf{y}_k}\mathcal{K}^T$$

where, $\mathbf{x}^a = [\mathbf{x}^T\ \mathbf{v}^T\ \mathbf{n}^T]^T$, $\boldsymbol{\mathcal{X}}^a = [(\boldsymbol{\mathcal{X}}^x)^T\ (\boldsymbol{\mathcal{X}}^v)^T\ (\boldsymbol{\mathcal{X}}^n)^T]^T$, λ=composite scaling parameter, L=dimension of augmented state, $\mathbf{P_v}$=process noise cov., $\mathbf{P_v}$=measurement noise cov., W_i=weights as calculated in Eqn. 15.

Figure 2: UKF Algorithm [8]

3.3. Propagation and Estimation Function

Given the initial states $\mathbf{x}_{0,T}$ of all the targets, a time window t_{span} and a list of the available sensors, the algorithm for propagating and estimating the target states includes the following steps:

1. Propagate all targets using Earth oblateness and drag models.
2. Propagate all the spacecraft in the constellation us-

ing Keplerian dynamics.

3. Compute the positions of the ground sensors in ECI throughout the time window, assuming that the axis of rotation of the Earth coincides with the z-axis of the ECI frame.
4. For each target, verify for each timestep the visibility from the ground network and the constellation.
5. For each target, build the measurement vector at each timestep.
6. For each target, use UKF to estimate the target state evolution. The model used in UKF neglects the atmospheric drag.
7. Iterate over all targets.

This algorithm is used to build up a function that maps the inputs to some meaningful outputs that are used to compute the performance metrics. These outputs are the simulated target state evolution vectors $\mathbf{x}_k(t)$, the estimated target state evolution vectors $\mathbf{x}_{est,k}(t)$, and the number of available sensors for each target $n_k(t)$, where k is an index going from 1 to N_t, with N_t number of targets. The data is then post-processed to obtain uptime with at least three sensors available, that is the percentage of time for which the target is visible to at least three or more optical sensors.

$$uptime_k = \frac{\sum_{k=0}^{N_k}(n(t_k) > 2)}{N_k} \tag{23}$$

where N_k is the number of timesteps.

3.4. Performance Metrics and Optimization Procedure

The performance metric used for the optimization is the (negative) average uptime for the target population:

$$cost = -\text{mean}_k\ uptime_k \tag{24}$$

This metric is chosen as three optical sensors are the minimum to cover the six state variables and estimate the target state accurately. This metric is only valid for estimating the constellation performance as long as the visibility is strictly correlated with the estimation error. This may not always be the case: although indeed when measurements are lacking it is not possible to estimate the target state accurately, three sensors may not be enough for accurate estimation, for instance due to geometric dilution of precision. The metric is taken as negative due to the definition of the optimization problem as a minimization problem. The cost function is then the function that maps the constellation parameters, given the inputs described in Section 3.3 and for a fixed number of constellation spacecraft, to the cost as defined above. In particular:

$$cost = f(p,\ N_{SAT},\ \mathbf{x}_{0,T},\ t_{span}) = f(p) \tag{25}$$

where $p = [N_{SC/ORB},\ N_o,\ \Omega_0,\ in,\ h]^T$ as described in Table 1. The optimization problem is then:

$$\min_p\ f(p) \tag{26}$$

subject to:

$$\begin{cases} N_o \times N_{SC/ORB} = N_{SAT} \\ 0 < \Omega_0 < \frac{\pi}{2} \\ 0 < in < \pi \\ 600\text{ km} < h < 1200\text{ km} \end{cases} . \tag{27}$$

Since the problem is highly nonlinear, due to the propagation of the nonlinear dynamics and the visibility constraints, the optimization routine that was chosen was the genetic algorithm as implemented in Matlab [9]. A genetic algorithm is a type of evolutionary optimization algorithm. In general, it initializes a random generation of parameter sets, calls the cost function for each, selects a subset of survivors within the generation based on the performance, and generates another generation of parameters based on the survivor set mimicking natural evolution [10]. The genetic algorithm is adventageous when dealing with nonlinear problems with mixed integer constraints due to its versatility, but the high number of calls of the cost function make it computationally expensive. The algorithm settings used for this work were $PopulationSize = 20$, $MaxStallGeneration = 8$, $MaxGenerations = 20$, $FunctionTolerance = 10^{-3}$.

4. Results

In this section the results for the constellation estimation function and the optimization are shown and analysed for some subsets of the parameter space. The objective is to compare the performance of the constellation to the ground network for some specific target and to retrieve useful information for guiding the preliminary design of a constellation of optical sensors.

4.1. Comparison with ground network

A simulation is carried on for approximately two orbital periods for a sun-synchronous target at 98 deg inclination and 700 km altitude. The constellation is constituted by one orbit with 32 spacecraft orbiting at 70 deg inclination and 1200 km altitude. The difference between the estimated position and the simulated position is well within 3 standard deviations as it can be seen from Figures 3a-3b, meaning that the UKF tuning was carried on correctly. It is also possible to see how the standard deviation alternates time windows of high reliability with a 100 to 400 m uncertainty with windows of exploding uncertainty.

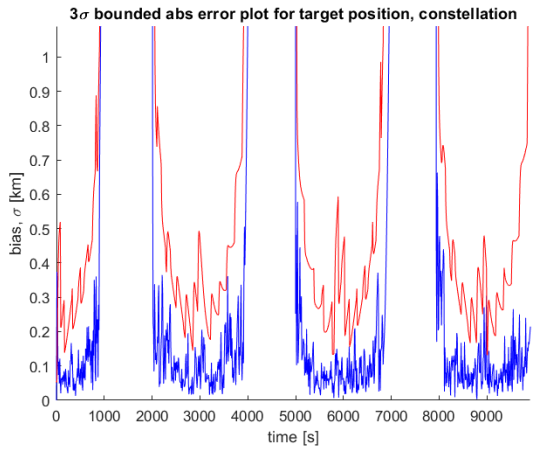

(a) 1 km scale

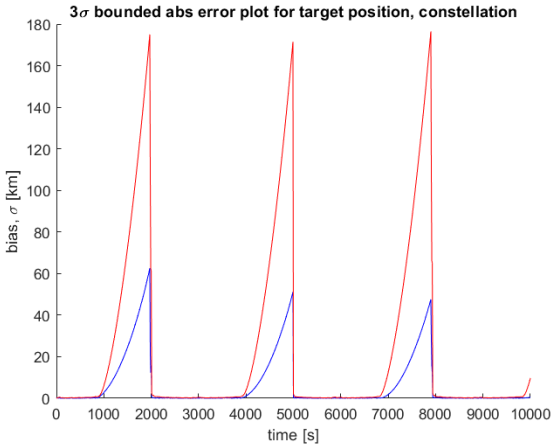

(b) 200 km scale

Figure 3: 3σ plot for position error and std deviation at two different scales. The position error is in blue, the 3σ curve in red.

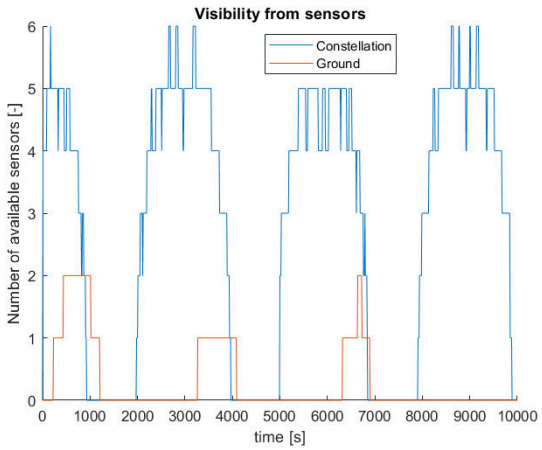

Figure 4: Available sensors against time for ground network and constellation

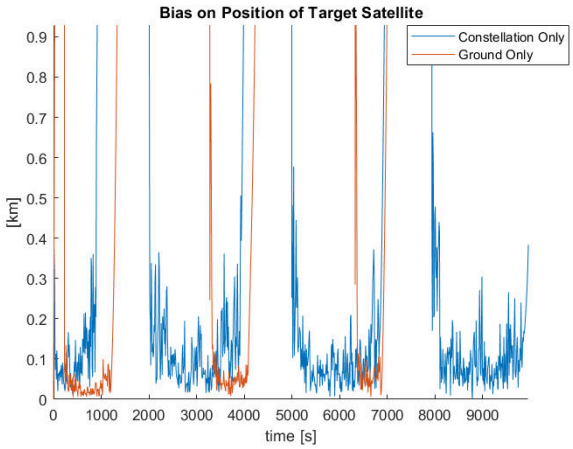

Figure 5: Position estimation error for ground network against constellation

This can be explained by looking at Fig. 4, where it can be seen that the uncertainty grows exponentially whenever no measurements are available. From the same figure it possible to see how the constellation is capable of observing the target for a much higher percentage of the time window despite having all the spacecraft on a single orbit. This yields beneficial effects, as the position is accurate for a higher percentage of the timespan as it can be seen from Fig. 5. Despite this, the same figure also shows the main disadvantage of relying on the constellation. When the measurements are available, the ground network outperforms the constellation despite having only one or two sensors at a time against four to six. This is attributable to the higher quality of information that a radar system delivers compared to an optical one, suggesting that one should be careful when choosing such systems for targeting LEO spacecraft.

4.2. Optimization Results

The optimization is carried on for two populations of 10 targets as defined in Section 2.1. The two cases will consequently be referred to as *random* and *SSO limited*. Fig. 6 shows the behaviour of the algorithm for *SSO limited* with $N_{SAT} = 20$. It is possible to see that the optimizer converges quite rapidly to a local minimum, but has difficulties decreasing further and it stalls at generation 16 as it has not found any significantly better solution for the past eight generations. This indicates that the problem is quite stiff, and finding a global minimum requires many more function calls and an higher capability of exploring the parameter space.

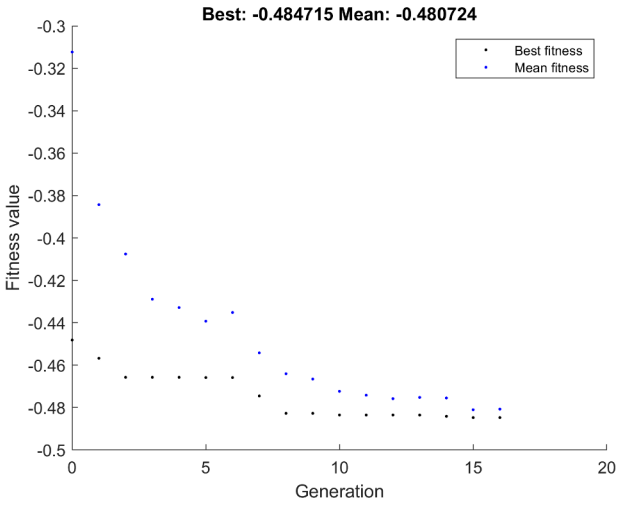

Figure 6: Minimum and average cost value against generation number, *SSO limited* population with $N_{SAT} = 20$.

Tables 3-4 show the results for the two populations for N_{SAT} between 12 and 24.

Table 3: Best parameters, *Random* population

$\mathbf{N}_{SAT}$ [-]	$\mathbf{N}_o$ [-]	$\mathbf{\Omega}_0$ [deg]	**in** [deg]	**h** [km]
12	3	291.30	20.85	1164
14	1	291.73	9.06	1115
16	1	234.14	13.58	1197
18	3	198.75	56.25	1177
20	1	291.44	11.38	1167
22	1	183.94	7.97	1140
24	3	303.55	27.32	1167

Table 4: Best parameters, *SSO limited* population

$\mathbf{N}_{SAT}$ [-]	$\mathbf{N}_o$ [-]	$\mathbf{\Omega}_0$ [deg]	**in** [deg]	**h** [km]
12	3	262.15	131.33	1128
14	1	279.71	163.92	1139
16	1	235.29	171.14	1199
18	3	263.20	122.88	1152
20	1	240.26	153.05	1199
22	1	225.71	141.82	1176
24	3	240.43	171.52	1183

It is possible to observe that there is some regularity in the sets of best parameters. First, the altitude is always near the upper bound of 1200 km. This is intuitive, as it is the configuration that guarantees geometrically the maximum visibility. Since in our model no dependency of the accuracy of the optical sensors on the range is introduced, we expect that such a results translates even when considering the average estimation error as the cost function for the optimization. In both cases, once a population is fixed the best RAAN and inclination values do not change much. If for the *SSO limited* population this can be explained by the narrow range of the targets orbital parameters, for a random population it is likely driven by the eclipse conditions imposed by the Sun, as the direction of Sunlight does not change much over three hours. Regarding the constellation geometry, the best number of orbits always seems to be odd. This means that even number of orbits likely do not yield a favourable ratio between the covered geometry and the number of spacecraft per orbital plane.

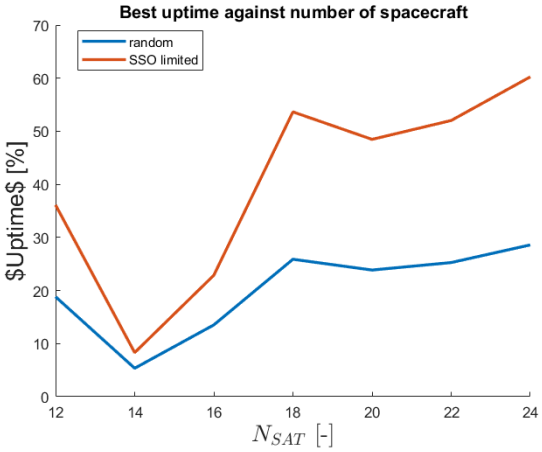

Figure 7: Best uptime value against number of spacecraft.

The most interesting results, however, can be found in Fig. 7. The plot shows the best average uptime with at least three sensors available against the number of spacecraft for the two populations. The behaviour of the two curves are very similar, meaning that how to best allocate the constellation spacecraft has some degree of independence with respect to the target population. In both cases, the visibility does not increase linearly with the number of spacecraft. This is because some number of spacecraft cannot be arranged in the best geometries given the constellation constraints. In these cases, the best configurations are those corresponding to a number of spacecraft divisible by three. Of course, if the increase in the number of spacecraft is very high, there can be an increase in the performance even if this divisibility condition does not apply, but from the perspective of the constellation designer this may be too expensive and not worth the effort. Finally, for the two target populations the uptime values are very different. When optimizing for a limited range of orbital parameters, it is possible to reach very good performance, as with around 60% coverage the parts that are missing are likely those that cannot be observed due to the Sun eclipse and not due to the constellation geometry. This follows intuition as it is more difficult to readily observe targets that are much more scattered, and therefore it is a

verification for the good functioning of the optimizer.

5. Conclusion

As more and more anthropogenic space objects are introduced in the space environment every year, potentially yielding an higher number of collisions, the need for a highly accurate space surveillance system for risk mitigation grows. Current ground based systems fare well for their accuracy and cost, but are not complete in terms of coverage and need high efforts in international cooperation to work effectively. In this paper, a potential solution of a constellation of spacecraft carrying optical payload was investigated. First, a methodology for modelling the constellation and evaluating numerically its performance was presented. To explore the advantages and limitations of such a system, a simulation for a single target object was carried on. The simulations confirmed the potential advantage of the constellation compared to a ground network of six radar stations spread over multiple continents in terms of coverage. Next, an optimization procedure was developed for finding the best constellation parameters in terms of number of available sensors. The results showed that it is possible to efficiently design the constellation to target specific objects or orbital regions and that the performance does not scale linearly with the number of spacecraft giving Walker-like constellation constraints.

In order to gain tools for designing such constellations or evaluating their contributions to a space surveillance network, much more research is required. The results of this study were limited both by the many simplifying assumptions and the limited available computing power used for performing the parametric analyses. Future research may investigate how the performance of the constellation depends on the constellation parameters for longer simulation times, for stricter and more realistic sensor assumptions, including for instance a dependency of the accuracy on the range or a limited field of view for the optical payload carried by the constellation satellites, for an higher number of target objects of different sizes, and using a model for the attitude of the constellation spacecraft.

References

[1] ESA. ESA's Space Environment Report 2023, 2023. URL https://www.esa.int/Space_Safety/ESA_s_Space_Environment_Report_2023. Last accessed 15 September 2023.

[2] EU SST. URL https://www.eusst.eu/. Last accessed 15 September 2023.

[3] ESA. Sapphire (Space Surveillance), 2012. URL https://www.eoportal.org/satellite-missions/sapphire-space-surveillance#sapphire-space-surveillance-mission-of-canada. Last accessed 15 September 2023.

[4] M. Guan, T. Xu, F. Gao, W. Nie, and H. Yang. Optimal walker constellation design of leo-based global navigation and augmentation system. *Remote Sensing*, 12(11), 2020. ISSN 2072-4292. doi: 10.3390/rs12111845. URL https://www.mdpi.com/2072-4292/12/11/1845.

[5] M. E. Awad, M. A. Sharaf, and E. Khatab. Visual contact between two earth's satellites. *American Journal of Applied Sciences*, 9:620–623, 2012.

[6] Renerpho. Phase angle diagram, 2019. URL https://commons.wikimedia.org/wiki/File:Phase_angle_explanation.png. Last accessed 15 September 2023.

[7] D. A. Vallado. Fundamentals of astrodynamics and applications. 1997.

[8] E. Wan and R. Van Der Merwe. The unscented kalman filter for nonlinear estimation. In *Proceedings of the IEEE 2000 Adaptive Systems for Signal Processing, Communications, and Control Symposium (Cat. No.00EX373)*, pages 153–158, 2000. doi: 10.1109/ASSPCC.2000.882463.

[9] Matlab. ga, 2023. URL https://uk.mathworks.com/help/gads/ga.html. Last accessed 15 September 2023.

[10] D. Simons. Evolutionary optimization algorithms. 2013.

2023-10-06

Optimal orbital configurations of spaceborne optical sensors constellations for space surveillance

D'Anniballe, Antonio

International Astronautical Federation (IAF)

D'Anniballe A, Felicetti L, Hobbs S. (2023) Optimal orbital configurations of spaceborne optical sensors constellations for space surveillance. In: IAC 2023 Congress Proceedings, 74th International Astronautical Congress (IAC) 2023, 2-6 October 2023, Baku, Azerbaijan https://dl.iafastro.directory/event/IAC-2023/paper/79933/